JMEPEG (2004) 13:32-38
DOI: 10.1361/10599490417560

1059-9495/$19.00

Effects of Different Metallurgical Processing on Microstructures and Mechanical Properties of Inconel Alloy 783

Longzhou Ma and Keh-Minn Chang

(Submitted 17 April 2002; in revised form 31 July 2003)

Different metallurgical processing, including the standard heat treatment, heat treatment without β aging, addition of high amount of Cr, and long-term isothermal exposure, was conducted on superalloy Inconel 783. For these processed materials, the tensile property and hardness at room temperature and stress relaxation behavior at 650 °C were examined. The testing results showed that isothermal exposure and heat treatment without β aging slightly enhanced the yield strength of alloy 783 at room temperature as well as all metallurgical processing in this study produced an identical stress relaxation behavior at 650 °C. The microstructure variation with different processing was analyzed using optical microscope, scanning electron microscopy (SEM), and transmission electron microscopy (TEM).

Keywords heat treatment, Inconel 783, microstructure, stress relaxation, tensile

1. Introduction

As a particular group of superalloy, the low coefficient of thermal expansion (CTE) iron-nickel based superalloys, such as Incoloy (Special Metals Corporation, Huntington, WV), alloy 903, 907, and 909, have been used in aircraft engine components to enhance the efficiency of air engines by controlling clearances between turbine or compressor blade tips and outer seals and shrouds in the past twenty years. Since increasing Cr content beyond 5.0 wt.% lowers Curie temperature and thereby increases CTE, most conventional low-CTE superalloys contain only a residual level of Cr. Consequently, these alloys are susceptible to stress accelerated grain boundary oxidation (SAGBO). With increasing the operation temperature of aircraft engine, the susceptibility to SAGBO strongly limits the applications of these high-strength and low-CTE alloys in the modern state-of-the-art air engine.[1] Recently developed γ-γ′-β three phase controlling Inconel alloy 783 (nominal composition of Ni-34Co-26Fe-5.4Al-3Nb-3Cr) is a result of the low-CTE superalloy development program aimed at improving the resistance to SAGBO, while maintaining the low CTE and high strength. Relative to the conventional superalloys such as Incoloy 903, 907, and 909, the uniqueness of alloy 783 in chemical composition is its high aluminum content (5.4 wt.%) to introduce β (NiAl-type) phase in addition to the formation of the strengthening phase, γ′ [Ni_3Al-type], in an austenitic matrix.

It has been reported that β phase was resistant to SAGBO-induced degradation such as sustained loading crack growth and stress rupture.[1-4] As a preliminary part of the research program to extensively evaluate the SAGBO resistance of alloy 783, the purpose of this study is to investigate the effect of different metallurgical processing, which includes the standard heat treatment, heat treatment without β aging, increasing of Cr content, and long-term isothermal exposure, on the microstructure, tensile properties, and hardness at room temperature, and stress relaxation behavior at elevated temperature. The results obtained in this study will aid in understanding the SAGBO-induced cracking behavior of alloy 783 in further research.

Longzhou Ma, Harry Reid Center for Environmental Studies, University of Nevada, Las Vegas, NV 89154; and **Keh-Minn Chang,** Department of Mechanical and Aerospace Engineering, West Virginia University, Morgantown, WV 26506. Contact e-mail: lma@unlv.nevada.edu.

2. Materials and Experimental Procedures

2.1 Materials and Metallurgical Processing

Commercially produced superalloy Inconel 783 used in this study was supplied by Special Metals Corporation, Huntington, WV, in the form of rolled strips. The nominal and analyzed chemical composition of these materials is listed in Table 1. As seen in Table 1, one piece of material contains a high content of Cr (5.56 wt.%). The blank samples with normal Cr and high Cr were cut from the deformed plates along the longitudinal orientation and were subjected to a standard heat treatment. This consisted of the following steps: (a) anneal at 1120 °C for 1 h and air cool, (b) age at 843 °C for 4 h and air cool, and (c) age at 718 °C for 8 h and furnace cool at 55 °C/h to 621 °C for 8 h and air cool. Step (b) will be referred to as β aging in the text, and step (c) will be referred as γ′ aging, which caused the strengthening phase γ′ to precipitate. To produce a microstructure essentially devoid of intergranular β phase, the second set of specimens with normal Cr content was heat-treated only using steps (a) and (c), omitting β aging. After the standard heat treatment, another set of specimens with normal Cr content were isothermally exposed at 500 °C for 3000 h in air. All samples were machined into dog-bone tensile specimens with a cross section of 3.18 × 3.18 mm, and an effective length of 44.45 mm. The microstructures developed through hot rolling and heat treatments were examined by an optical microscope and scanning electron microscope (SEM).

Table 1 Chemical Composition of Experimental Alloy 783 (wt.%)

Element	High-Cr Alloy 783	Normal Alloy 783	Nominal Composition
Ni	28.59	28.21	28.0
Fe	25.59	24.88	Balance
Co	31.41	34.39	34.0
Al	5.28	5.32	5.4
Nb	2.96	3.11	3.0
Ti	0.18	0.32	0.2
Cr	5.56	3.24	3.0

Samples were sectioned and mounted for polishing following standard laboratory procedures. Kalling's reagent, which contains 6 g $CuCl_2$ + 100 ml HCl + 100 ml H_2O + 100 ml CH_3OH, was used to reveal the microstructure. Metallographic pictures were taken under a Leitz Laborlux 12 ME optical microscope (Leica Micro-system Inc., Bannockbum, IL), to which a CCD camera and a PC computer were attached to catch the image digitally. A Hitachi S-750 SEM (Hitachi, Tokyo, Japan) was used to examine the fracture surface after tensile testing and β precipitates after heat treatments. TEM samples were prepared by a twinjet thinning apparatus using a solution of 10% perchloric acid in methanol at 28 V and −50 °C, and samples were observed with a Phillips EM400 microscope (FEI Company, Hillsboro, OR).

2.2 Tensile Property and Stress Relaxation Measurement

The tensile test was conducted at room temperature in an MTS material testing servo-hydraulic system (MTS System Corporation, Eden Prairie, MN). The tensile rate was kept at 0.02 mm/s for all specimens. To measure the creep resistance of alloy 783 subjected to different metallurgical processing, a tensile stress relaxation test was performed at 650 °C. Following the testing procedure as illustrated in ASTM E 328-86-1991, the stress relaxation test was carried out at a tensile strain rate of 0.02 mm/s and 650 °C. It has been reported the elongation of alloy 783 is 37% at 650 °C.[4] Therefore, once the specimen started plastic deformation attaining a strain of about 4.5%, the crosshead displacement of the MTS was stopped. The position of the crosshead was maintained with a feedback loop while the load was allowed to drop. The data acquisition system monitored the time and load variation. A quartz heater mounted on the MTS provides a uniform temperature across the specimen with a temperature fluctuation of ±5 °C.

3. Results

3.1 Microstructure

The optical microstructures under different treatment conditions are shown in Fig. 1. Since the recrystallization temperature of alloy 783 is 1115 °C, all samples display an isotropic microstructure with a similar grain size of ASTM 5-7. The residual strain structure introduced by hot rolling has been eliminated by annealing. All samples subjected to the standard heat treatment and isothermal exposure showed the continuous grain boundary networks and lots of isolated particles. However, the sample subjected to heat treatment without β aging exhibited only the isolated particles, and the continuous grain boundary profiles could not be revealed. This observation indicates that the introduction of β aging during heat treatment has a remarkable effect on grain boundary morphology. Figure 2 displays the SEM image for β precipitate morphology of as-polished samples. Since body centered cubic (bcc) β [NiAl-type] phase is incoherent with the face centered cubic (fcc) matrix in alloy 783, SEM micrographs of samples subjected to standard heat treatment and isothermal exposure showed that numerous plate-like β precipitate networks formed the clear grain boundary profiles during heat treatment, as seen in Fig. 2.

With a solvus temperature of 1140 °C for the β phase, Fig. 2 shows a few of inter- and intragranular globular β particles, which formed during processing but were not dissolved completely during annealing. These globular β precipitates actually correspond to the isolated particles, as seen in Fig. 1. All samples subjected to the heat treatment including β aging demonstrate an identical morphology of the β precipitate. In contrast, the continuous plate-like β precipitates and grain boundary profile could not be observed for sample subjected to the heat treatment without β aging, and only observable were the isolated globular β particles.

3.2 Tensile Property and Hardness at Room Temperature

Table 2 shows the results of tensile property and hardness tests at room temperature for specimens subjected to different treatments. Only yield strength is pronouncedly different. The isothermally exposed specimen shows the highest yield strength ($\sigma_{0.2}$). Also, the specimen without β aging exhibits the higher yield strength than as-produced and high-Cr specimens. All specimens display the comparable ultimate strength (σ_b), elongation (δ) and hardness, except for no β aged specimen showing slightly higher hardness and lower elongation than other specimens.

3.3 Tensile Stress Relaxation

One example of the tensile stress relaxation testing results at 650 °C is shown in Fig. 3. As seen in Fig. 3(a), the as-produced specimen was loaded by tension with a strain rate of 0.02 mm/s at 650 °C. When the tensile stress reached about 720 MPa, the specimen produced yielding. Further applying the tension, plastic deformation took place. As soon as the plastic strain reached 4.5%, the movement of the crosshead of the MTS was stopped, and then the position of crosshead was held by the monitor system. During holding, the stress would drop as shown in Fig. 3(a). Figure 3(b) illustrates the stress drop as a function of time during holding. The portion of stress drop in Fig. 3(b) was extracted for conversion to the form of strain rate versus stress according to the transformation relationship of stress versus time and strain rate versus stress variation as shown in Eq 1 and 2.[5] The processed result is displayed in Fig. 4, wherein the strain rate as a function of stress is plotted. Figure 5 represents the stress relaxation behaviors of all specimens. The fact that all curves of strain rate versus stress almost overlap each other suggests that all specimens demonstrate the identical stress relaxation behaviors at 650 °C, and the creep resistance of alloy 783 is independent of the different treat-

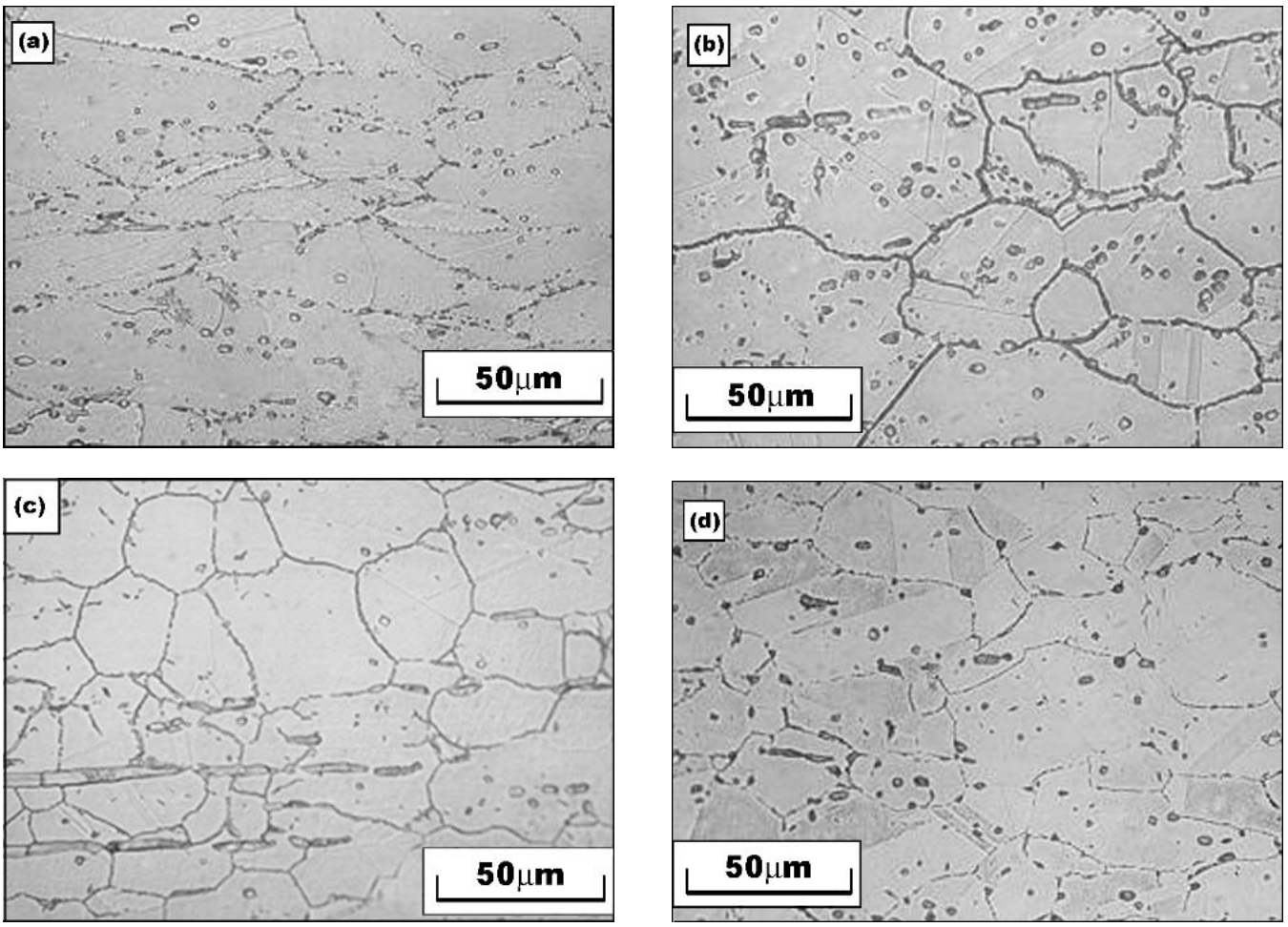

Fig. 1 Optical microstructure of alloy 783 subjected to different processing showing a similar grain size of ASTM 5-7: **(a)** no β aging, **(b)** as-produced, **(c)** high Cr, **(d)** isothermally exposed

Table 2 Tensile Property and Hardness at Room Temperature

Sample	$\sigma_{0.2}$, MPa	σ_b, MPa	δ, %	Hardness, HRC
No β aging	883	1233	18.5	41
As-produced	853	1225	25.9	36
High Cr	817	1216	24.2	31
Isothermally exposed	953	1236	20.2	34

ments including the heat treatment with/without β aging, high Cr addition, and prolonged isothermal exposure.

The power law relationship between stress and time during stress relaxation is:

$$\sigma = \omega \cdot t^m \quad \text{(Eq 1)}$$

where σ is stress, ω is a material constant, t is time, and m is a factor.

The relationship between plastic strain rate, $\dot{\varepsilon}_P$ and stress change is:

$$\dot{\varepsilon}_P = B \frac{\partial \sigma}{\partial t}, \quad \text{(Eq 2)}$$

where B is a constant.

4. Discussion

Alloy 783 primarily consists of three phases, γ′ (Ni_3Al-type), β (NiAl-type), and γ austenitic phase. After the standard heat treatment including annealing, β aging, and γ′ aging, the volume fraction of γ′ and β phase respectively is approximately 24% and 15% according to CALPHAD computational simulation.[6] The γ′ phase in alloy 783 nucleates homogeneously and grows uniformly to provide the alloy strength. The fine γ′ precipitates usually are too small to be visible by an optical microscope. On the contrary, the β phase nucleates and grows preferentially along the region with high density of dislocation such as grain boundaries. Since the β precipitate is incoherent with the austenitic matrix in alloy 783, SEM observation of the as-polished sample shows that the β precipitate forms the clear grain profiles during β aging. It has been re-

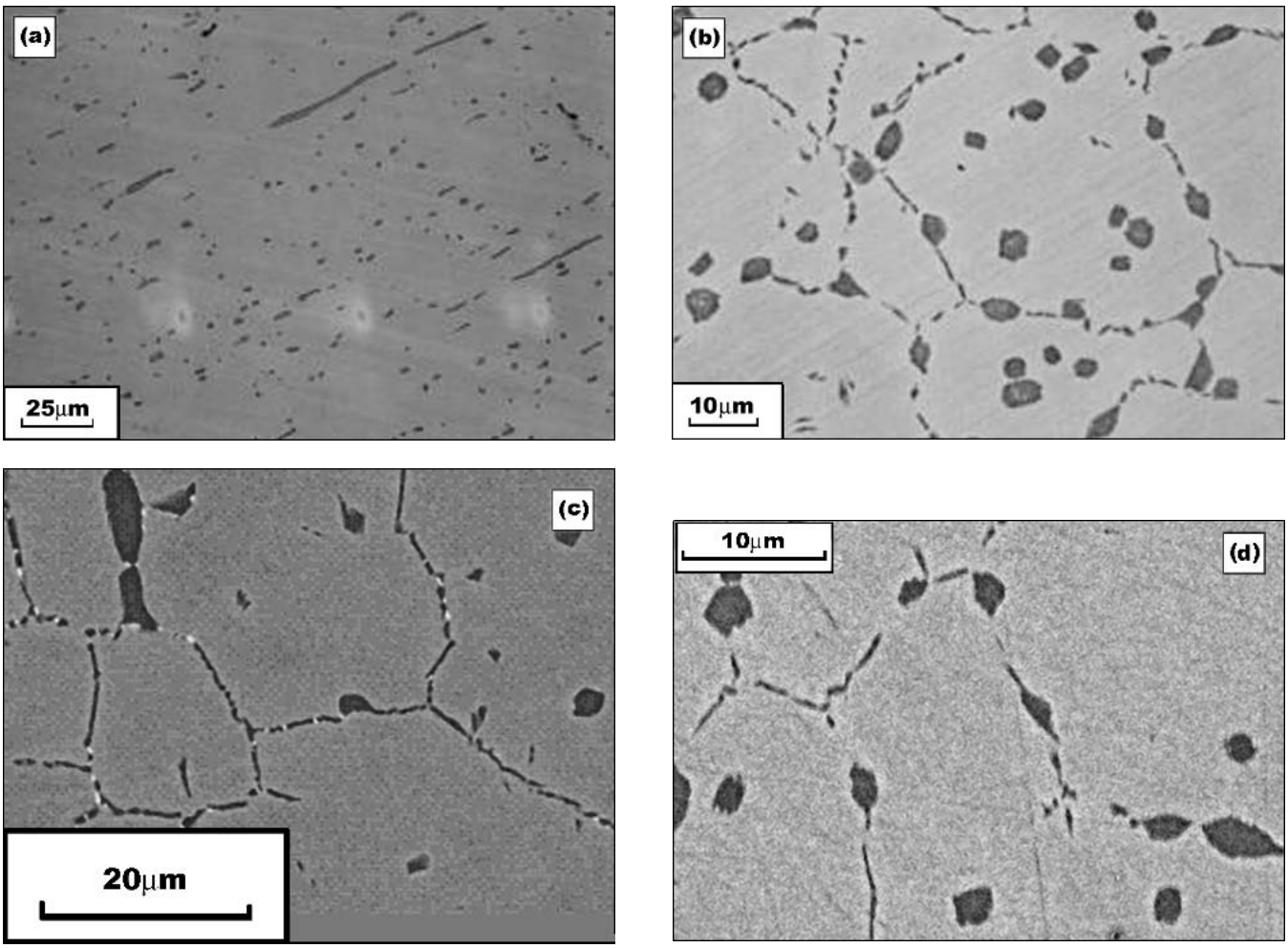

Fig. 2 SEM micrograph of β precipitate of alloy 783 subjected to different processing showing that the plate-like β precipitates formed the grain boundary profile in **(b)**, **(c)**, and **(d)**: **(a)** no β aging showing the isolated globular β particles, **(b)** as-produced, **(c)** high Cr, **(d)** isothermally exposed

ported that the chemical composition of β (NiAl-type) phase in alloy 783 determined by SEM/EDX analysis contained approximately 30% Ni, 24% Co, 15% Fe, and 31% Al by atomic percentage.[4]

Since Co and Fe would occupy Ni lattice site, β phase [(NiFeCo) Al- type] could be Al-rich. Studies have shown that the Al-enriched β phase during oxidation can manifest itself as a protective alumina scale (Al_2O_3) to prevent further oxidation at elevated temperature (597-897 °C).[7-9] Also, early studies have indicated that the β phase in alloy 783 could play an important role in enhancing the resistance to SAGBO-induced cracking.[1,10] Relative to as-produced and high-Cr specimens, the specimen subjected to the heat treatment without β aging displays higher strength and lower elongation. Since alloy 783 is a γ′-β-γ three-phase-controlling alloy, the fact that heat treatment without β aging would reduce the fraction of β precipitates and in turn increase the fraction of γ′ may contribute to the increase of yield strength of the specimen without β aging. As shown in Table 2, addition of high Cr in alloy 783 lowers the strength. This is likely to be associated with the fact that the increase of Cr resulted in a decrease of Co content as seen in Table 1 since Co was considered as a balance element while experimental alloys were prepared. It has been reported that Co had a stronger solidification strengthening effect than Cr in superalloys.[11]

Another important finding in this study is that thermal exposure generates the highest strength compared with other treatments such as heat treatment with/without β aging and addition of high amount of Cr. Actually, the effect of prolonged isothermal exposure on mechanical properties of superalloys has received an extensive concern recently, since the components of aircraft engine made of superalloys have to be exposed up to 500 °C for at least 30 000 h under service condition. Radavich found that the prolonged thermal exposure of superalloy 718 at 650 °C for 800 h in air would introduce the over aging effect, which could increase the size of γ″ (Ni_3AlNb) precipitate, and thereby decrease mechanical properties.[12] Mannan and deBarbadillo also reported that the prolonged exposure for alloy 718, 783, and 909 would decrease the high-temperature elongation by about 10-20%.[4] To understand the effect of thermal exposure on mechanical properties of alloy 783, as-produced and exposed samples were examined under TEM. Figure 6(a) shows the morphology of the γ′ precipitate in as-produced sample. Numerous γ′ particles are coherent

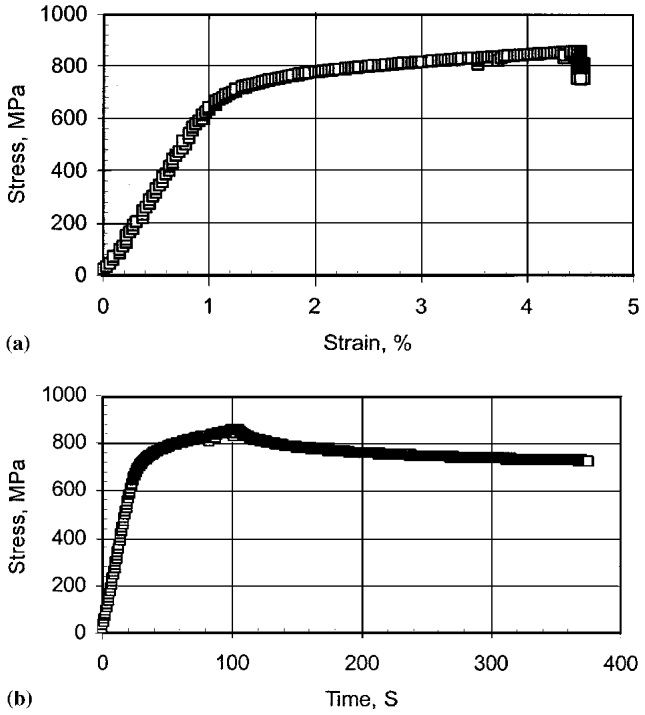

Fig. 3 Measurement of stress relaxation behavior of as-produced specimen at 650 °C: **(a)** stress versus strain, **(b)** stress versus time

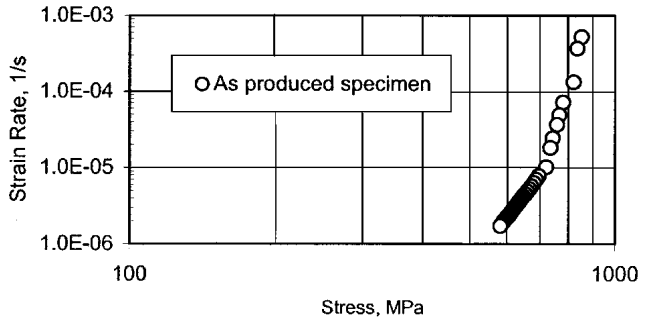

Fig. 4 Stress relaxation behavior of as-produced specimen at 650 °C

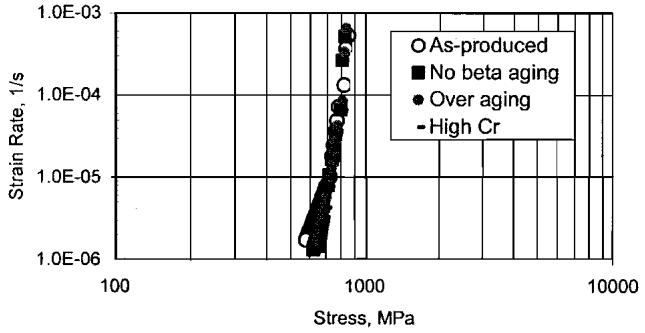

Fig. 5 Comparison of stress relaxation behaviors of alloy 783 subjected to different processing at 650 °C

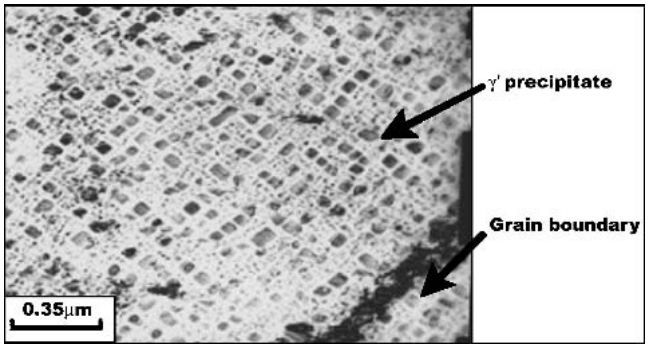

Fig. 6 TEM micrograph of γ′precipitate in as-produced sample

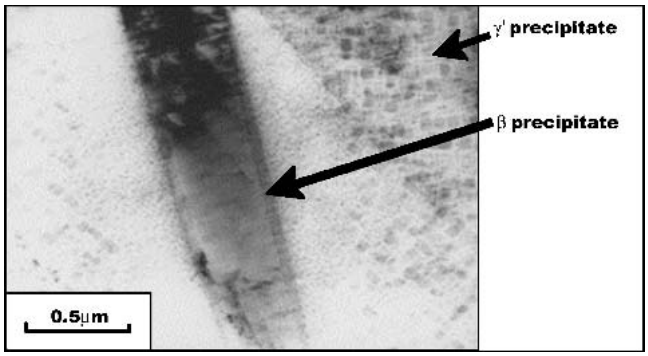

Fig. 7 TEM micrograph of β and γ′ precipitates in as-produced sample

with matrix and homogenously precipitate. The γ′ particles are cubodial with an average size of 43 nm. Figure 7 shows that the plate-like β precipitates are incoherent with matrix and much bigger than γ′ particles. High-magnification observation shows that the plate-like β phase in as-produced material is clean and essentially devoid of any internal precipitation as seen in Fig. 8(a). However on 3000 h isothermal exposure at 500 °C, the β phase was found to contain numerous γ′ (Ni_3Al-type) precipitates, which were spherical with an average particle size of 12 nm as shown in Fig. 8(b). Studies have already indicated that the β phase in the Ni-Al intermetallic system could transform to γ′ phase and Ni_5Al_3 on exposure in the temperature ranging from 500 to 700 °C.[13]

Thus, it is reasonable to find γ′ particles present within the β phase on isothermal exposure at 500 °C for 3000 h. The β phase in as-produced material is hardened by solidification strengthening with Co and Fe and also by point defect due to non-equiatomic composition. However, the β phase in the isothermally exposed materials is also dispersion strengthened by γ′ precipitates. This may be essentially responsible for the increase of yield strength in exposed specimens.

The fracture surfaces of all tensile specimens show typically ductile fracture. Figure 9 presents two examples of SEM micrograph of fracture surface for the as-produced and non-β aged specimen. As seen in Fig. 9(a), many ductile cups and dimples appear on the fracture surface, indicating that lots of plastic deformation occurred during tensile testing. Under such fracture conditions, material usually shows the high ductility. In contrast, the fraction of ductile cup seems to decrease in the specimen without β aging, corresponding to a lower elongation, as shown in Fig. 9(b). The residual globular β particles

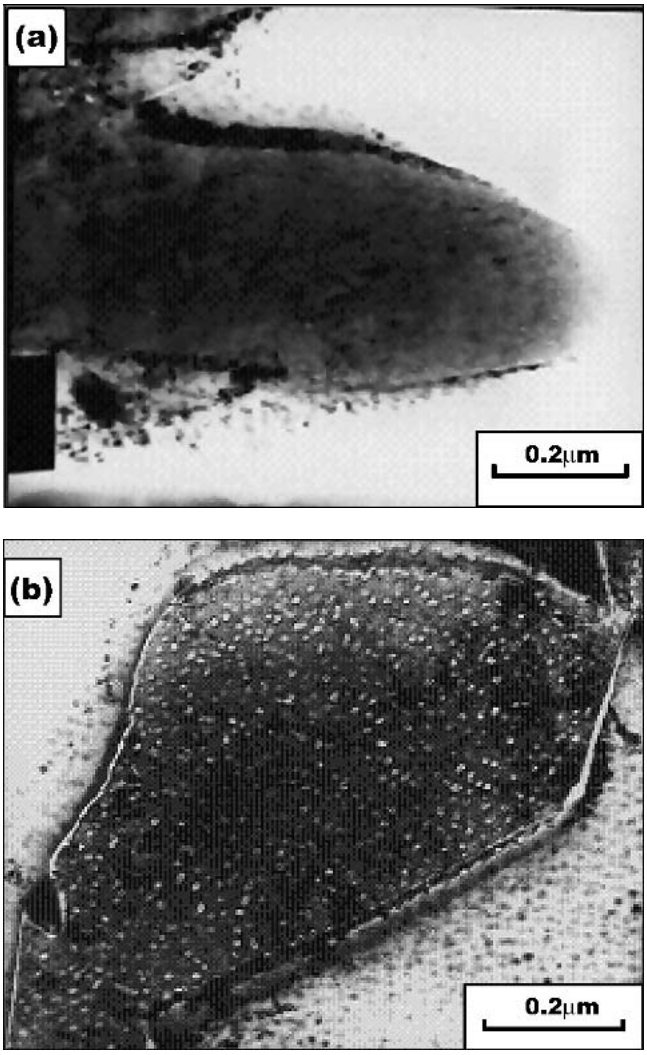

Fig. 8 Bright field TEM micrograph of β and γ′ precipitate: **(a)** as-produced sample showing no internal precipitation within β phase, and **(b)** Isothermally exposed sample showing γ′ precipitates within β phase

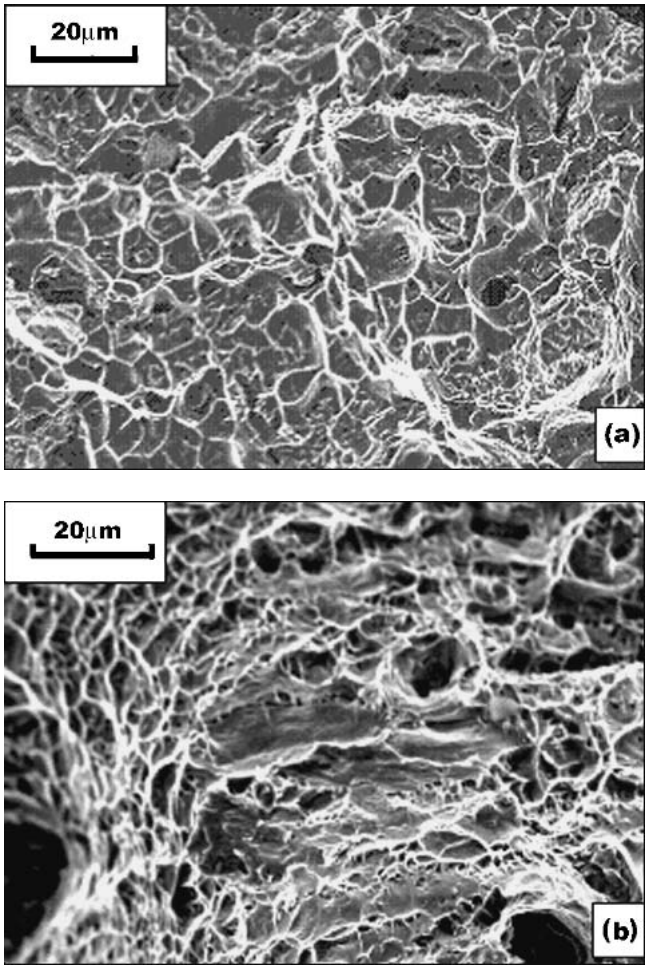

Fig. 9 SEM micrograph of tensile fracture surface: **(a)** as-produced specimen, and **(b)** isothermally exposed specimen

may act as a fracture nucleation core, and some big holes were left on the surface after fracture.

As displayed in Fig. 5, all metallurgical processing including heat treatment with/without β aging, high Cr addition, and isothermal exposure have no significant effect on stress relaxation behavior of alloy 783 at 650 °C. Essentially, the stress relaxation behavior is a dislocation- movement-induced creep deformation process, which is associated with the thermal-activation process. Therefore, an Arrhenius thermal activation equation can be used to correlate the strain rate with stress and temperature as shown in Eq 3[5]:

$$\dot{\varepsilon}_P = A\,\sigma^n \exp\left(\frac{-Q}{RT}\right), \qquad \text{(Eq 3)}$$

where $\dot{\varepsilon}_P$ is strain rate, n is stress exponent, A is a material constant, R is the gas constant, Q is creep activation energy, and T is absolute temperature. When temperature is fixed, $\dot{\varepsilon}_P$ has a linear relationship with stress in the log-log coordinate system. As seen in Fig. 5, the linear relationship between strain rate and stress is evident within experimental scatter. Usually the stress exponent n, which is a function of internal structure and chemical composition of material, determines the creep resistance of material. In this study, the almost overlapped stress relaxation curves suggest these experimental materials, subjected to the different metallurgical processing, have an identical value of n and comparable creep resistance. The microstructure and addition of high Cr cannot significantly affect the creep resistance of alloy 783. This finding is important for studying the fatigue crack growth or sustained loading crack growth behavior of alloy 783 at elevated temperature in air, since the identical stress relaxation behavior of alloy 783 with different treatments and high Cr content allow one to consider only the environmental factor, such as SAGBO, and rule out the creeping effect on crack growth.[10,14,15]

5. Conclusions

As preliminary research of the extensive research program aimed at evaluating the resistance of alloy 783 to SAGBO-

induced cracking, this study identified the microstructure variation, tensile property and stress-relaxation behavior of alloy 783 subjected to different metallurgical processing. The testing and analyzed results suggest the following conclusions, which play a very important role to assist understanding the SAGBO-induced crack propagation behavior of alloy 783 in the next research phase:

1) Different metallurgical processing for alloy 783 including heat treatment with/without β aging, addition of high content of Cr, and long-term isothermal exposure generates an isotropic microstructure with a similar grain size of ASTM 5-7.
2) Heat treatment with β aging allows the continuous plate-like β phase network to precipitate along grain boundaries. Addition of a high content of Cr and isothermal exposure cannot affect morphology of β precipitate. The continuous β precipitates did not appear in the specimen without β aging, except for a few annealing-residual globular β particles.
3) Alloy 783 subjected to an isothermal exposure at 500 °C for 3 000 h can lead to the over aging effect, which causes the spherical γ′ phase to precipitate within β phase.
4) All metallurgical processing in this study produces an identical stress relaxation behavior at 650 °C.
5) All metallurgical processing in this study cannot significantly affect the tensile properties at room temperature. The slight increase of yield strength for prolonged specimen exposure is perhaps related to the internal formation of γ′ phase within β phase.

Acknowledgments

This work was supported by the Air Force Office of Scientific Research, Arlington, VA, under Grant No. F49620-99-1-0274 and the West Virginia Experimental Program to Stimulate Competitive Research (EPSCOR) program. Appreciation is also expressed to Special Metals Corporation, Huntington, WV, for supplying the experimental materials.

References

1. J.S. Smith and K.A. Heck: " Development of Low Thermal Expansion, Crack Growth Resistant Superalloy" in *Superalloys 1996,* R.D. Kissinger, D.J. Deye, D.L. Anton, A.D. Cetel, M.V. Nathal, T.M. Pollock, and D.A. Woodford, ed., TMS, Seven Springs, PA, 1996, pp. 91-100.
2. K.A. Heck, J.S. Smith, and R.L. Smith: " Inconel Alloy 783: An Oxidation Resistant, Low Expansion Superalloy for Gas Turbine Applications" in *International Gas Turbine and Aeroengine Congress & Exhibition,* Birmingham, UK, 1996, pp. 1-8.
3. K.A. Heck, D.F. Smith, M.A. Holderby, and J.S. Smith: "Three-Phase Controlled Expansion Superalloys with Oxidation Resistance" in *Superalloy 1992,* S.D. Antolovich, R.W. Stusrud, R.A. Mackay, D.L. Anton, T. Khan, R.D. Kissinher, and D.L. Klarstorm, ed., TMS, Seven Springs, PA, 1992, pp. 217-26.
4. S. Mannan and J. deBarbadillo: "Long Term Thermal Stability of INCONEL Alloy 783" in *International Gas Turbine and Aeroengine Congress & Exhibition,* Stockholm, Sweden, 1998, pp. 1-10.
5. G.E. Dieter: *Mechanical Metallurgy,* McGraw Hill Press, New York, NY, 1986, pp. 309-10.
6. M.S. Seehra, A. Manivannan, C. Cionca, L. Ma, and K-M. Chang: "Effects of Heat Treatments and Thermimechanical Processing on The Beta and Gamma Phase in INCONEL 783 Alloy" in *Advanced Technologies for Superalloy Affordability,* K-M. Chang, S.K. Srivastava, D.U. Furrer, and K.R. Bain, ed., TMS, Warrendale, PA, 2000, pp. 141-48.
7. E.W.A. Young and J.H.W. de Wit: "The Application of Rutherord Backscattering Spectrometry on the Study of High Temperature Corrosion Processes With Special Emphasis on the Oxidation of β NiAl" in *International Congress on Metallic Corrosion,* 9th, National Research Council, Toronto, Canada, 1984, pp. 50-53.
8. P.A. van Manen, E.W.A. Young, D. Schalkoord, C.J. van der Wekken, and J.H.W. de Wit: "The Influence of Y on the Structure and Growth Mechanism of Alumina Scales," *Surface and Interface Analysis,* Vol. 12, 1988, pp. 391-96.
9. E.W.A. Young, J.C. Riviere, and L.S. Welch: "Growth Mechanism of Al_2O_3 Scales Developed of FeCrAl Alloys," *Appl. Surf. Sci.,* 1988, *31,* pp. 370-74.
10. L. Ma, K-M. Chang, S.K. Mannan, and S.J. Patel: "Effects of NiAl-β Precipitates on Fatigue Crack Propagation of INCONEL Alloy 783 Under Time-Dependent Condition With Various Load Ratio," *Scripta Mater.,* 2003, *48,* pp. 551-57.
11. G. Chen: *Metallurgy of Superalloy,* Metallurgical Industry Press, China, 1988, pp. 3-10 (in Chinese).
12. J.F. Radavich and A. Fort: "Effects of Long-Time Exposure in Alloy 625 at 1200 F, 1400 F and 1600 F" in *Superalloy 718, 625 and Various Derivatives,* E.A. Loria, ed., TMS, Warrendale, PA, 1994, pp. 635-47.
13. L.M. Roberston and C.M. Wayman: "Ni_5Al_3 and the Nickel-Aluminum Binary Phase Diagram," *Metallography,* 1984, *17,* pp. 41-47.
14. L. Ma, K-M. Chang, S.K. Mannan, and S.J. Patel: "Effect of Prolonged Isothermal Exposure on Elevated-Temperature, Time-Dependent Fatigue-Crack Propagation in INCONEL Alloy 783," *Metall. Trans. A,* 2002, *33A,* pp. 3465-78.
15. L. Ma, K-M. Chang, and S.K. Mannan: "Oxide-Induced Crack Closure: An Explanation for Abnormal Time-Dependent Fatigue Crack Propagation Behavior in INCONEL Alloy 783," *Scripta Mater.,* 2003, *48,* pp. 583-88.